Eur Biophys J (2002) 31: 559–562
DOI 10.1007/s00249-002-0245-z

BIOPHYSICS LETTER

Derek Marsh

Membrane water-penetration profiles from spin labels

Received: 19 March 2002 / Revised: 3 June 2002 / Accepted: 1 July 2002 / Published online: 13 September 2002

Abstract Spin label hyperfine splittings in mixtures of protic and aprotic solvents are used to obtain association constants $K_{A,h}$ for hydrogen bonding to oxazolidine nitroxides. With the Onsager approach to account for the variation in local dielectric constant, these results are used to determine the effective penetration profile of water into fluid phospholipid membranes, from recent electron paramagnetic resonance (EPR) studies on phospholipids spin-labelled systematically down the *sn*-2 chain. Water penetration is appreciable, depends on chain unsaturation, and is strongly affected by cholesterol.

Keywords Hydrogen bonding · Nitroxide · Polarity profile · Local dielectric constant · Water permeation

Introduction and theoretical background

The polarity profiles across lipid membranes are fundamental not only to the transport of water and polar solutes, but also to the energetics of insertion of proteins into membranes. In a recent paper, the current author characterized transmembrane polarity profiles in fluid lipid bilayers by the isotropic hyperfine splitting constants, $a_o{}^N$, of phospholipids spin-labelled in the *sn*-2 chain (Marsh 2001). To translate these polarity profiles into profiles for the permeation of water requires taking into account the contribution from variations in the local dielectric environment. In this communication, we attempt to do this by means of an effective local dielectric constant that depends on the water concentration.

Measurements of isotropic hyperfine couplings of spin labels in aprotic solvents of different dielectric constant have demonstrated the importance of the Onsager reaction field. This varies with the polarization of the solvent according to $(\epsilon-1)/(\epsilon+1)$, where ϵ is the dielectric constant (Griffith et al. 1974). Studies with binary mixtures of protic and aprotic solvents have demonstrated the importance also of hydrogen bonding to the nitroxide:

$$\mathrm{R^1R^2NO + PH} \overset{K_{A,h}}{\longleftrightarrow} \mathrm{R^1R^2NO---HP} \tag{1}$$

which is determined by the association constant, $K_{A,h}$, and the molar concentration of proton donor, [PH] (Gagua et al. 1978; Al-Bala'a and Bates 1987). From the law of mass action, the isotropic ^{14}N hyperfine coupling constant of the spin label is then given by the sum of these contributions (e.g., see Marsh 2002):

$$a_o^N = \frac{a_{o,o}^{\varepsilon=1} + K_v \frac{\varepsilon-1}{\varepsilon+1} + a_{o,h}^N K_{A,h}[\mathrm{PH}]}{1 + K_{A,h}[\mathrm{PH}]} \tag{2}$$

where $a_{o,o}^{\varepsilon=1} = 1.385$ mT and $K_v = 0.064$ mT for the oxazolidine-*N*-oxy spin-labelled lipids (Griffith et al. 1974). Here $a_{o,h}^N$ is the isotropic coupling constant of the hydrogen-bonded spin label. Al-Bala'a and Bates (1987) showed that the value of this does not depend on the dielectric constant of the solvent. Equation 2 assumes that exchange between H-bonded and non-H-bonded nitroxides is rapid compared with the difference in their isotropic hyperfine splittings.

In mixtures of solvents with dielectric constants ϵ_v and ϵ_h, where the latter is for the proton donor PH, the net dielectric constant depends on composition according to the Onsager relation (Onsager 1936; Marsh 2002):

$$\begin{aligned}\frac{\varepsilon-1}{\varepsilon} = {} & \left(\frac{\varepsilon_h-1}{\varepsilon_h}\right)\left(\frac{2\varepsilon+1}{2\varepsilon_h+1}\right)\left(\frac{2\varepsilon_h+n_h^2}{2\varepsilon+n_h^2}\right)^2 \frac{[\mathrm{PH}]}{[\mathrm{PH}]_o} \\ & + \left(\frac{\varepsilon_v-1}{\varepsilon_v}\right)\left(\frac{2\varepsilon_v+n_v^2}{2\varepsilon+n_v^2}\right)\left(1-\frac{[\mathrm{PH}]}{[\mathrm{PH}]_o}\right)\end{aligned} \tag{3}$$

where $[\mathrm{PH}]_o$ is the molarity of the pure hydrogen-bonding solvent (i.e., $[\mathrm{H_2O}]_o = 55.5$ M), and n_h and n_v are the refractive indices of the polar and apolar solvents, respectively. For the polar solvent, the dipolar

D. Marsh (✉)
Max-Planck-Institut für biophysikalische Chemie,
Abteilung Spektroskopie, 37070 Göttingen, Germany
E-mail: dmarsh@gwdg.de

contribution is assumed to dominate over that of the polarizability. Equation 3 represents the dielectric constant in mixtures of polar and apolar solvents reasonably adequately, which the Clausius-Mossotti relation, for instance, does not (Marsh 2002). Combination of Eqs. 2 and 3 therefore yields the dependence of a_o^N on hydrogen donor concentration in binary solvent mixtures.

Spin labels in mixed solvents

Figure 1 gives data for the oxazolidine-*N*-oxy spin-labelled fatty acid 16-SASL, at 10^{-4} M concentration in mixtures of protic and aprotic solvents. Solvents were of analytical or spectroscopic grade and dried over a molecular sieve. Water was double distilled. Conventional EPR spectra of the spin label in the solvent mixtures were recorded at 30 °C on a Varian Century Line 9 GHz spectrometer at 5 mW microwave power, 0.01 mT modulation amplitude, and with a field scan of 5 mT. Single-component EPR spectra indicated solvent miscibility at all compositions. The hyperfine coupling constant, a_o^N, measured directly from the isotropic spectra, is plotted in Fig. 1 against the concentration of proton-donor, either water or trifluoroethanol (TFE).

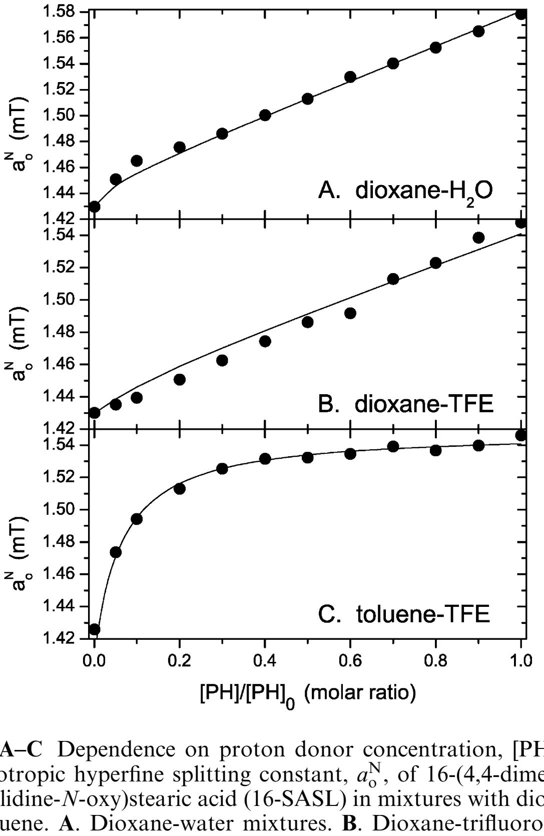

Fig. 1A–C Dependence on proton donor concentration, [PH], of the isotropic hyperfine splitting constant, a_o^N, of 16-(4,4-dimethyl-oxazolidine-*N*-oxy)stearic acid (16-SASL) in mixtures with dioxane or toluene. **A**. Dioxane-water mixtures. **B**. Dioxane-trifluoroethanol mixtures. **C**. Toluene-trifluoroethanol mixtures. The *solid line* in **C** is the fit of Eqs. 2 and 3 with $K_{A,h} = 1.0 \pm 0.1$ M^{-1} and the parameters given in the text. The *solid lines* in **A** and **B** are fits of Eqs. 3 and 4, with a linear dependence on [PH] and a polarity contribution appropriate to dioxane (see text)

For mixtures with dioxane, the isotropic hyperfine splitting increases almost linearly with increasing concentration of water or TFE (Fig. 1A and B). This indicates only weak hydrogen bonding to the nitroxide and is possibly linked with the "anomalous" behaviour of dioxane as a low-dielectric solvent (Reddoch and Konishi 1979). This anomaly is most evident in the atypically high values of a_o^N in dioxane, relative to those in apolar solvents of similar dielectric constant, possibly due to partial stabilization of the boat conformation by the reaction field of neighbouring polar molecules. Presumably, also dioxane itself takes part in hydrogen bonding with protic solvents. In contrast, TFE clearly forms hydrogen bonds with the nitroxide in mixtures with the apolar solvent toluene (see Fig. 1C). Fitting Eqs. 2 and 3 to the data of Fig. 1C yields an association constant for hydrogen bonding to the oxazolidine nitroxide of $K_{A,h} = 0.96 \pm 0.14$ M^{-1}. Correspondingly, the isotropic hyperfine coupling of the hydrogen-bonded complex is $a_{o,h}^N = 1.548 \pm$ 0.003 mT, very close to that of neat TFE (viz., 1.546 mT). Values of $a_{o,o}^{\varepsilon=1}$ and K_v given above for oxazolidine spin labels (Griffith et al. 1974), together with dielectric constants $\epsilon_v = 2.379$, $\epsilon_h = 24.3$ and refractive indices $n_v = 1.4961$, $n_h = 1.2907$ (Weast 1980), were used for this estimate.

In Fig. 1A and B, the almost-linear concentration dependence implies also that the polarity-dependent contribution to a_o^N is smaller for mixtures with dioxane. This is again associated with the anomalous behaviour of dioxane and requires that a_o^N in dioxane be used as the low-dielectric calibration point (cf. above), giving values of $a_{o,o}^{\varepsilon=1} = 1.419$ mT and $K_v = 0.028$ mT (cf. Gagua et al. 1978). The solid lines in Fig. 1A and B represent this polarity correction, plus a linear dependence on proton donor concentration:

$$a_o^N = a_{o,o}^{\varepsilon=1} + K_v \frac{\varepsilon - 1}{\varepsilon + 1} + K_h \frac{[PH]}{[PH]_o} \qquad (4)$$

which is a limiting form of Eq. 2 for $K_{A,h}[PH] < < 1$, where $K_h = a_{o,h}^N K_{A,h} [PH]_o$ (cf. Gagua et al. 1978). From non-linear least-squares fits of Eqs. 3 and 4, the resulting linear dependences on proton concentration are $K_h = 0.134 \pm 0.002$ mT and 0.096 ± 0.003 mT for dioxane-water and dioxane-TFE mixtures, respectively. The effects of both proton donors are thus comparable, at least to within a factor that corresponds to the ratio of molarities of the two solvents.

Unfortunately, water is only very sparingly soluble in toluene or other conventional apolar solvents. Hence, a direct determination of its hydrogen bonding with 16-SASL in these solvents is not possible. However, comparison of the data given in Fig. 1A and B suggests that the association constant for hydrogen bonding with TFE in toluene, $K_{A,h} = 1.0$ M^{-1}, might reasonably represent that for water in a hydrophobic environment. Correspondingly, a value of $a_{o,h}^N = 1.576$ mT is taken from measurements with 16-SASL in pure water. This information, together with the hyperfine parameters appropriate to the oxazolidine-*N*-oxy spin labels, then allows estimation of the local water concentration in membranes from EPR measurements with spin-labelled phospholipids (Marsh 2001). Values of $\epsilon_h = 80$, $n_h = 1.3288$ for water and $\epsilon_v = 2$, $n_v = 1.43$ for the hydrocarbon chains can then be used to obtain values of [H_2O] and ϵ_{loc} in Eqs. 2 and 3 that are consistent with the experimental measurements of a_o^N. This is done numerically.

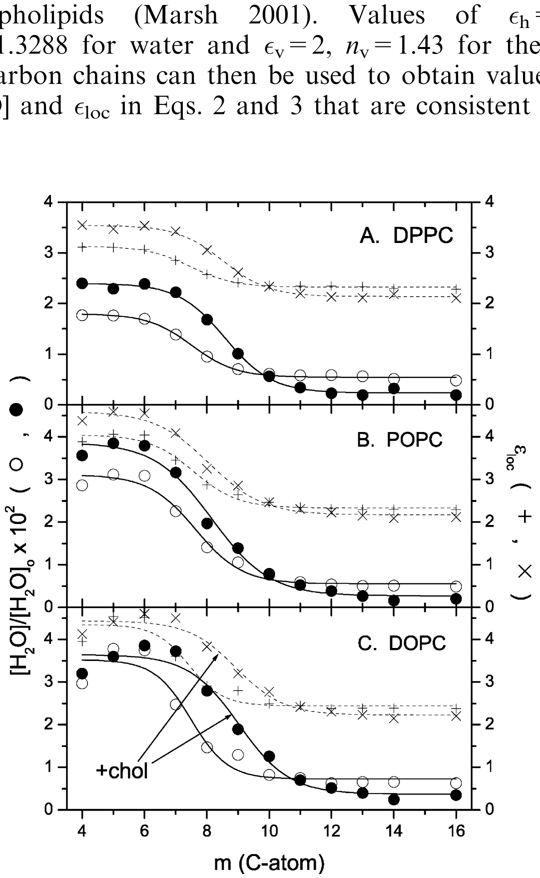

Fig. 2 Water permeation profile in fully hydrated fluid bilayer membranes of **A** dipalmitoylphosphatidylcholine, **B** 1-palmitoyl-2-oleoylphosphatidylcholine and **C** dioleoylphosphatidylcholine, with (*solid circles*) and without (*open circles*) 50 mol% cholesterol. Effective values of the water concentration, [H_2O], are deduced from Eqs. 2 and 3 by using spin label EPR data (Marsh 2001), and are plotted against the C-atom position, *m*, in the *sn*-2 chain of phosphatidylcholine. *Crosses* give the effective local dielectric constant, ϵ_{loc}, deduced from Eq. 3, for membranes with (*diagonal cross*) and without (*upright cross*) 50 mol% cholesterol. *Solid lines* are fits of Eq. 5 to the values of [H_2O] versus *m*, with the fitting parameters given in Table 1. *Dashed lines* are corresponding fits for ϵ_{loc}

Lipid spin labels in membranes

Figure 2 gives the effective water penetration profiles into bilayer membranes of dipalmitoyl-, 1-palmitoyl-2-oleoyl- and dioleoylphosphatidylcholines, with and without cholesterol, that are obtained from EPR spectra of 1-acyl-2-[*m*-(4,4-dimethyloxazolidine-*N*-oxyl)]stearoyl-*sn*-glycero-3-phosphocholine (*m*-PCSL) at probe amounts. The original EPR data are taken from Marsh (2001) for measurements in the fluid L_α-phase of the fully hydrated phospholipid membranes. After the correction for the variation in local dielectric constant, the trough-like profile that characterizes the positional dependence of a_o^N is still preserved. It is adequately described by the Boltzmann sigmoidal form:

$$[PH] = \frac{[PH]_1 - [PH]_2}{1 + e^{(m-m_o)/\lambda}} + [PH]_2 \tag{5}$$

where $[PH]_1$ and $[PH]_2$ are the limiting values of the proton donor concentration at the lipid headgroup and terminal methyl ends of the chain, respectively, and λ is an exponential decay constant. The chain position $m = m_o$ corresponds to the maximum gradient of the profile, at which $[PH] = 0.5([PH]_1 + [PH]_2)$. The solid lines in Fig. 2 represent non-linear least-squares fits of Eq. 5 to the data with and without cholesterol. Figure 2 also gives values of the effective local dielectric constant that are deduced from Eq. 3. The resulting profiles are similar to those for the effective water concentration, despite the non-linear nature of Eq. 3, and they yield similar values for m_o and λ.

Equation 5 is identical in form to that used previously to describe the a_o^N profile (Marsh 2001). Because the present analysis is based directly on effective concentrations, the interpretation in terms of a two-phase distribution between outer and inner membrane regions is even more appropriate. In this model, the free energy of transfer, $(m\text{–}m_o)k_BT/\lambda$, increases linearly with distance $m\text{–}m_o$ from the dividing plane at $m = m_o$. Table 1 gives the parameters characterizing this distribution for

Table 1 Parameters characterizing the effective water permeation profile (see Eq. 5) of fully hydrated fluid lipid membranes with and without 50 mol% cholesterol[a]

Lipid	$[H_2O]_1/[H_2O]_o$ (%)	$[H_2O]_2/[H_2O]_o$ (%)	m_o	λ
DMPC	2.04 ± 0.03	0.41 ± 0.03	7.77 ± 0.06	0.37 ± 0.05
DMPC + chol	2.45 ± 0.09	0.22 ± 0.08	8.7 ± 0.2	0.8 ± 0.2
DPPC	1.80 ± 0.03	0.55 ± 0.02	7.52 ± 0.08	0.70 ± 0.07
DPPC + chol	2.40 ± 0.04	0.24 ± 0.03	8.59 ± 0.08	0.75 ± 0.07
POPC	3.1 ± 0.1	0.55 ± 0.07	7.6 ± 0.2	0.7 ± 0.1
POPC + chol	3.9 ± 0.2	0.27 ± 0.09	8.2 ± 0.2	0.9 ± 0.2
DOPC	3.5 ± 0.2	0.7 ± 0.1	7.5 ± 0.3	0.6 ± 0.2
DOPC + chol	3.6 ± 0.1	0.4 ± 0.1	9.0 ± 0.2	0.8 ± 0.2

[a] Values of $[H_2O]/[H_2O]_o$ are deduced from Eqs. 2 and 3 using spin-label EPR data (Marsh 2001), as in Fig. 2

a series of saturated and unsaturated fluid phosphatidylcholine membranes, with and without cholesterol. The water permeation profiles display a dependence on membrane lipid composition similar to that deduced previously from the isotropic hyperfine constants (see Marsh 2001). Cholesterol deepens the hydrophobic trough by increasing water permeation at the headgroup end of the chains and reducing it in the middle of the membrane. Chain unsaturation increases water permeation at the headgroup part of the chains, hence lessening the effect of cholesterol in this region.

Although the water permeation profiles are qualitatively similar to those deduced from the original isotropic hyperfine couplings, there are quantitative differences. Both m_o and λ are decreased by up to 15%, relative to the values originally reported (Marsh 2001). Thus the hydrophobic trough is wider and the sides are steeper. The largest increase in width of the trough is by 2–2.5 CH_2 segments, for unsaturated lipids with cholesterol.

The most notable feature of Table 1 is that the effective water concentrations are quite significant at the headgroup ends of the chains. For saturated chains these are 2–2.5%, and for unsaturated chains 3–3.5% of that in pure water. This translates to effective bulk water concentrations in the range 1–2 M, depending on degree of unsaturation and cholesterol content. Non-vanishing water concentrations are found also in the middle of membranes not containing cholesterol, effectively 0.2–0.4 M, depending to some extent on degree of chain saturation. To put these effective bulk concentrations in context, a comparison with the effective molarity of a methylene group is appropriate. In fluid lipid membranes, this quantity is in the region of 51.3 M as compared with 55.5 M for pure water (e.g., see Marsh 1990). Thus the numbers in Table 1 approximately represent the effective mole fraction (in %) of water in the different parts of the hydrophobic region of the membrane.

The effective membrane water concentrations given in Table 1 are considerably higher than the solubility of water in bulk hydrocarbons. For fluid hexadecane, the water partition coefficient is 0.64×10^{-4} (Schatzberg 1963, 1965). The absolute accuracy of the water concentrations derived from spin labels depends directly on the value taken for $K_{A,h}$. In so far as this is representative of the hydrogen bonding of water to the spin label in membranes, the concentrations derived should reflect the free water concentration at that particular depth in the membrane. The polar nature of the nitroxide and its hydrogen bonding capabilities are thereby taken into account automatically. The bulk of the spin label attached to the lipid chain may cause steric perturbations in the membrane environment that are greater than the local disturbances of solvent packing at the spin-label site in the solutions used to measure $K_{A,h}$. This could lead to higher estimates of local free water concentration than in the unperturbed membrane regions remote from the spin label. However, this difference from a bulk solvent should be small in fluid lipid bilayers, especially at the higher temperatures (up to 70 °C) to which the spin label measurements extend. Note also that this effect is likely to be similar at all positions of the nitroxide, and therefore not to affect the shape of the water permeation profiles derived.

Acknowledgements The author thanks Frau B. Angerstein for skillful technical assistance.

References

Al-Bala'a I, Bates RD Jr (1987) Medium effects on ESR spectra in studies of hydrogen-bonded transient solvent-solute complexes. J Magn Reson 73:78–89

Gagua AV, Malenkov GG, Timofeev VP (1978) Hydrogen-bond contribution to isotropic hyperfine splitting constant of a nitroxide free-radical. Chem Phys Lett 56:470–473

Griffith OH, Dehlinger PJ, Van SP (1974) Shape of the hydrophobic barrier of phospholipid bilayers. Evidence for water penetration in biological membranes. J Membr Biol 15:159–192

Marsh D (1990) Handbook of lipid bilayers. CRC Press, Boca Raton, Fla

Marsh D (2001) Polarity and permeation profiles in lipid membranes. Proc Natl Acad Sci USA 98:7777–7782

Marsh D (2002) Polarity contribution to hyperfine splittings of hydrogen-bonded nitroxides. J Magn Reson 157:114–118

Onsager L (1936) Electric moments of molecules in liquids. J Am Chem Soc 58:1486–1493

Reddoch AH, Konishi S (1979) The solvent effect on di-*tert*-butyl nitroxide. A dipole-dipole model for polar solutes in polar solvents. J Chem Phys 70:2121–2130

Schatzberg P (1963) Solubilities of water in several normal alkanes from C_7 to C_{16}. J Phys Chem 67:776–779

Schatzberg P (1965) Diffusion of water through hydrocarbon liquids. J Polym Sci C 10:87–92

Weast RC (ed) (1980) Handbook of chemistry and physics, 61st edn. CRC Press, Boca Raton, Fla